


The involvement of mitochondrial fission in maintenance of the stemness of bone marrow mesenchymal stem cells

Xiaorong Feng¹, Wenjing Zhang^{1,2}, Wen Yin¹ and Y James Kang^{1,2} 

¹Regenerative Medicine Research Center, Sichuan University West China Hospital, Chengdu 610041, China; ²Memphis Institute of Regenerative Medicine, University of Tennessee Health Science Center, Memphis, TN 38163, USA

Corresponding author: Y James Kang. Email: ykang7@uthsc.edu

Impact statement

How to maintain the stemness of bone marrow mesenchymal stem cells (BMSCs) in cultures is a long-standing question. The present study found that mitochondrial dynamics affects the stemness of BMSCs in cultures and the retaining of mitochondrial fission enhances the stemness of BMSCs. This work thus provides a novel insight into strategic approaches to maintain the stemness of BMSCs in cultures in relation to the clinical application of bone-marrow stem cells.

Abstract

Mitochondrial dynamics, a complicated cellular process consisting of mitochondrial fusion and fission, has been suggested to be involved in regulating the stemness of bone marrow mesenchymal stem cells (BMSCs). This study was undertaken to explore the relationship between mitochondrial dynamics and the maintenance of BMSCs' stemness. Rat BMSCs were treated with fibroblast growth factor 2 (FGF2) and epithelial growth factor (EGF) to induce differentiation. Mitochondrial dynamics was determined by mitochondrial length observed by confocal microscope and DLP1 (a protein promoting mitochondrial fission), OPA1 (a protein promoting mitochondrial fusion) expression revealed by Western blotting analysis. BMSCs' stemness was determined by flow cytometry and osteogenic/adipogenic

differentiation ability. We found that in the process of BMSCs differentiation, mitochondrial length was increased, along with a decreased protein level of DLP1 and an increased protein level of OPA1 in the mitochondria, indicating a shift toward mitochondrial fusion in BMSCs during differentiation. Notably, when the mitochondrial fission was inhibited by Mdivi-1, the stemness marker, CD90, was decreased along with the reduction of DLP1 expression. Under the same condition, the potential of BMSCs to be induced into adipocytes or osteocytes was decreased. Correspondingly, when BMSCs were treated with tyrphostin A9, a reagent promoting mitochondrial fission by increasing DLP1, the stemness marker, CD54, was increased with an increased potential of BMSCs to be induced into adipocytes or osteocytes. Hence, our results demonstrated that mitochondrial fission contributed to the maintenance of BMSCs' stemness.

Keywords: Bone marrow mesenchymal stem cells, stemness, maintenance, mitochondrial fission, DLP1, tyrphostin A9

Experimental Biology and Medicine 2019; 244: 64–72. DOI: 10.1177/1535370218821063

Introduction

Bone marrow mesenchymal stem cells (BMSCs) are adult stem cells, possessing self-renewal capability and multiple differentiation potential.¹ Therefore, BMSCs have been extensively studied in relation to regenerative medicine.² In general, BMSCs are quiescent cells due to their low proliferative activity. Under pathological conditions, BMSCs proliferate rapidly and differentiate to functional cells to repair the injured tissues.^{3,4} BMSCs are widely used in tissue engineering because of their lower immunogenicity and tumorigenicity in comparison with other stem cells.⁵

However, BMSCs cultured *in vitro* have the tendency to differentiate spontaneously,^{6–8} jeopardizing their clinical application. Hence, it is necessary to gain a practical understanding of how to maintain the stemness of BMSCs in cultures.

A number of factors regulate the self-renewal and differentiation of stem cells, including nuclear transcription factors,⁹ cell cycle proteins,¹⁰ metal ions, and growth factors.^{11,12} Mitochondrial dynamics (fusion and fission) are also indicated as being involved in the regulation of the stemness of stem cells.^{13,14} For instance, the asymmetrical segregation of mitochondria controls

the mammosphere-forming capacity of human mammary stem-like cells during their division. Specifically, daughter cells with a greater proportion of young mitochondria grow into a larger population of mammospheres, and those with lesser young segregation arrive at a decreased number of mammospheres. Furthermore, the ability of the mammary stem-like cells to form mammospheres is decreased after treatment with Mdivi-1, a small molecule inhibitor of DLP1 used for selectively and reversibly inhibiting mitochondrial fission,¹⁴ indicating a possible involvement of mitochondrial fission in the maintenance of stemness.

The present study was undertaken to specifically address the relationship between mitochondrial fission and the maintenance of BMSCs' stemness. With the approach of either promoting or inhibiting mitochondrial fission, we found that mitochondrial fission contributed to the maintenance of BMSCs' stemness.

Materials and methods

Animal

Sprague-Dawley (SD) rats, aged five to seven days, were purchased from a state government-approved animal facility (DaShuo, Chengdu, China). The rats were kept in cages under standard laboratory conditions and given rat chow

and allowed free access to water. All experimental procedures were approved by the Sichuan University Animal Care and Use Committee in accordance with the Principles of Laboratory Animal Care regulated by the National Society for Medical Research.

Cell culture and treatment

BMSCs were prepared as described before.¹⁵ Briefly, after carefully removing the skin and muscle of the hind limbs, the complete bone marrow cells were flushed from femur and tibia using a 1 mL syringe containing Dulbecco's modified Eagle's medium-low glucose (DMEM-L; Gibco, USA) supplemented with 10% fetal bovine serum (FBS; Natocor, AR). Then bone marrow cells were divided into two groups, control and the other group treated with growth factors, fibroblast growth factor 2 (FGF2; 3339-FB-025, Abcam, USA) and epithelial growth factor (EGF; 3214-EG-100, Abcam). Cells were then plated into flasks or wells and incubated in a cell incubator containing 5% CO₂ at 37°C. Media were replaced every 2–3 days. When cells grew to 70% confluence, they were washed twice with phosphate-buffered saline (PBS) and treated with 0.25% trypsin (Gibco) in 1 mmol/L EDTA (Sigma-Aldrich, USA). After being resuspended in serum-supplemented media, cells were counted, and plated to 25 cm² flask

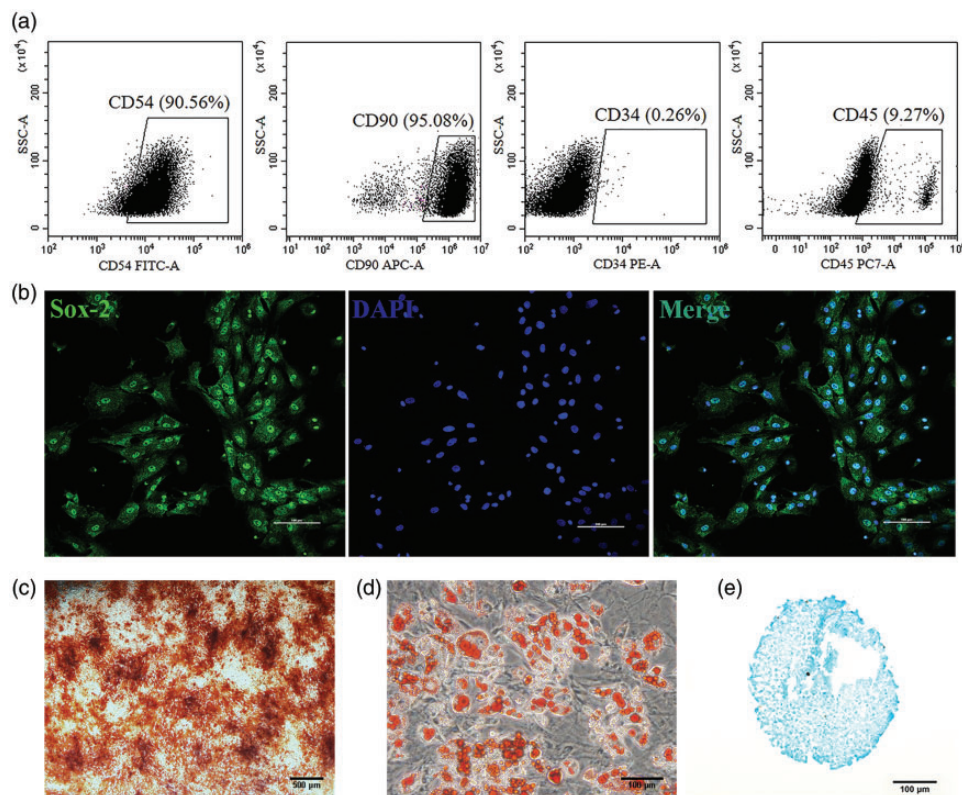


Figure 1. Isolated BMSCs with high purity and inducibility. (a) Determination of the positive (CD54, CD90) and the negative (CD34, CD45) surface markers of BMSCs by flow cytometry; (b) representative images of fluorescently stained Sox-2; nuclei were stained with DAPI (blue). Scale bars represent 100 μ m, original magnification $\times 200$. (c) Induction of BMSCs into osteocytes by culturing the cells in the osteogenic induction media for 14 days, visualized by Alizarin red S staining. Scale bar represents 500 μ m, original magnification $\times 40$. (d) Induction of BMSCs into adipocytes by culturing the cells in the adipogenic induction media for 21 days, visualized by Oil Red O staining. Scale bar represents 100 μ m, original magnification: $\times 200$. (e) Chondrogenic induction of BMSCs by culturing the cells in the induction media for 27 days, visualized by Alcian blue staining. Scale bar represents 100 μ m, original magnification $\times 200$. (A color version of this figure is available in the online journal.)

($5\text{--}7 \times 10^5$ cells). The third passage was used only for further experiments. For determination of the role of mitochondrial fission in stemness maintenance, BMSCs were treated with 50 $\mu\text{mol/L}$ Mdivi-1 for 6 h to inhibit mitochondrial fission or 1 $\mu\text{mol/L}$ tyrphostin A9 (TA9) for 24 h to promote mitochondrial fission before being harvested.

Flow cytometry

Around 2×10^4 cells were harvested and centrifuged for 5 min at 4°C . Fluorescein-conjugated antibodies, anti-CD54 (1:100; 554969, BD Biosciences, USA), anti-CD90 (1:100; 561409, BD Biosciences), anti-CD34 (1:20; sc-7324, Santa Cruz, USA), and anti-CD45 (1:100; 561588, BD Biosciences), were selected as demonstrated by previous studies and then coincubated with cells at room temperature for 30 min.^{1,16–22} After washing three times and centrifuging for 5 min at 4°C , cells were resuspended with 300 μL PBS and analyzed using flow cytometry (Becton, Dickinson and Company, Franklin Lakes, NJ, USA).

Immunofluorescence staining

BMSCs were seeded at approximately 60% confluence on coverslips. After being rinsed with PBS and fixed with freshly prepared 4% paraformaldehyde (PFA; Thermo Fisher, USA), cells were permeabilized with 0.1% Triton X-100 (Sigma-Aldrich) and incubated with 3% bovine serum albumin (Cell Signaling Technology, USA) for 1 h. Then, cells were incubated overnight at 4°C with Sox-2 antibody (1:200; ab75485, Abcam). After rinsing with PBS, cells were incubated in the dark with an Alexa Fluor 488 conjugated secondary antibody (1:1000; A11001, Thermo Fisher) for 1 h and briefly incubated with DAPI at room temperature. Finally, a confocal microscope (Nikon Ti A1, Japan) was used to determine the fluorescence intensity in BMSCs. Sox-2 and DAPI fluorescent images were captured at $\times 200$ magnification using a microscope (Nikon Ti A1).

Mitochondria imaging

Cells were adhered to coverslips before coincubation with MitoTracker Green (Invitrogen, USA) according to the manufacturer's instructions. In brief, freshly prepared MitoTracker Green in dimethyl sulfoxide (DMSO) was added to the culture to give a final concentration of 1 $\mu\text{mol/L}$ and incubated for 30 min before imaging. Cells were kept in the dark with a constant temperature of 37°C , then washed three times with FBS-free DMEM-L. Live images of mitochondria were captured by a confocal microscope equipped with oil immersion objective lens $60\times$ (λ_{ex} : 488 nm; λ_{em} : 515–530 nm). The changes in mitochondrial length were assessed according to a procedure published previously.²³ In brief, images were taken in a blinded way and at least 30 cells were counted in three independent experiments. Mitochondrial length was measured using Image J software. To be specific, images were extracted to grayscale, inverted to show mitochondria-specific fluorescence as black pixels, then sharpened and set for threshold to optimally resolve individual cells to estimate mitochondrial length. As the majority of

mitochondrial mass forms an interconnected “network” in BMSCs, and that one end of the network is often in the perinuclear region which makes the image difficult to resolve, thus, the resolvable length was always reported.

Isolation of mitochondria

Mitochondria were isolated according to a procedure published previously.²⁴ Cells were washed three times with PBS and scraped. The harvested cells were resuspended and centrifuged at 600g for 5 min at 4°C . Then, cells were resuspended again with 1 mL of ice-cold modified self-timed execution (MSTE) buffer (10 mmol/L Tris base, 0.07 mol/L sucrose, 0.21 mol/L D, L-mannitol, 0.5 mmol/L EGTA, 1 mmol/L EDTA, pH 7.4) and homogenized using a Dounce homogenizer. The homogenate was centrifuged at 600g for 5 min at 4°C . Supernatant was collected and centrifuged at 1000g for 5 min at 4°C . Then, supernatant was collected again and centrifuged at 7000g for 10 min at 4°C . Finally, the mitochondrial fraction was resuspended in 1 mL of MSTE buffer and washed, followed by centrifuging at 10,000g for 10 min at 4°C , the final deposit being the mitochondrial pellet.

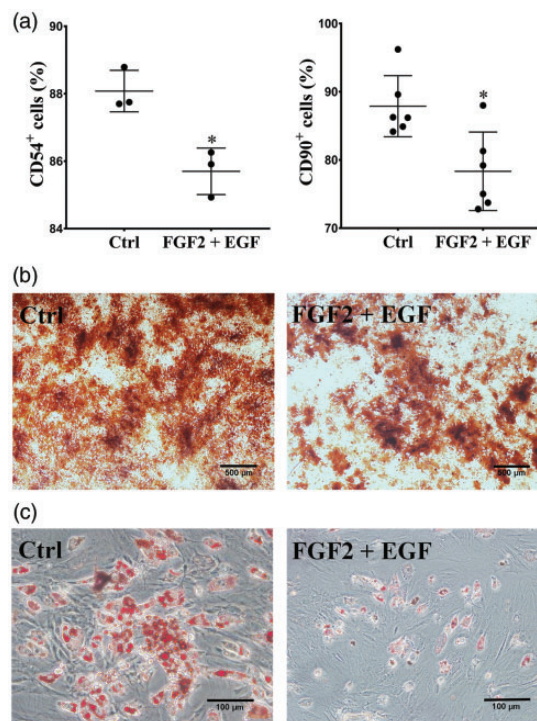


Figure 2. FGF2 and EGF induced differentiation of BMSCs. BMSCs were divided into two groups, control and FGF2 + EGF (treated with 5 ng/mL FGF2 and 10 ng/mL EGF for three passages). (a) Quantification of the fluorescence intensity of stemness markers (CD54 and CD90) of BMSCs by flow cytometry. Each dot represents one independent experiment. Bar graph values are mean \pm SEM. *Significantly different from the control group ($P < 0.05$). (b) Osteogenic induction of BMSCs detected by Alizarin red S staining. Scale bars represent 500 μm , original magnification $\times 40$. (c) Adipogenic induction of BMSCs detected by Oil Red O staining. Scale bars represent 100 μm , original magnification $\times 200$. (A color version of this figure is available in the online journal.)

Western blotting

Equal amounts of mitochondrial fraction (20 μg) from each group were separated by 10% SDS-PAGE. All proteins were transferred onto a polyvinylidene difluoride membrane (Bio-Rad, USA) using an electrophoretic transfer machine. Primary antibodies were listed as follows: DLP1 (1:1000; 611112, BD Biosciences), OPA1 (1:1000; 612606, BD Biosciences), and ATPB (1:1000; ab170947, Abcam). After incubation with primary antibodies overnight at 4°C, cells were washed three times for 10 min each by TBST. Then, cells were washed again following incubation with secondary antibodies for 1 h at room temperature. Proteins were visualized by chemiluminescence (Bio-Rad) and analyzed by IPP 6.0 (Image-Pro Plus 6.0, Media Cybernetics, USA).

Alizarin Red S and Oil Red O staining

BMSCs were seeded in six-well plates at a density of 3×10^5 cells/well. Cells were induced toward osteogenic differentiation or adipogenic differentiation for 21 days. After being washed with PBS and fixed with 10% formaldehyde at room temperature for 10 min, the cells were

incubated with 0.1% Alizarin Red S or 0.5% Oil Red O solution (Cyagen, USA) at room temperature for 20 min. After being washed with PBS three times, images were taken using an inverted phase-contrast microscope (Nikon, Tokyo, Japan).

Alcian blue staining

The 2.5×10^5 cells were cultured in a 15-mL centrifuge tube and induced to chondrogenic differentiation for 27 days. Then, cells were fixed in 4% PFA for 30 min at room temperature and rinsed three times with PBS. They were then progressively dehydrated at 4°C in sucrose (10%, 20% and 30% in PBS). Tissues were snap-frozen in OCT compound (Sakura Tissue-Tek). Tissue sections of 10 μm thickness were cut and stained with 1% Alcian blue (Cyagen) for 30 min at room temperature. After washing three times, photomicrographs (Nikon 80i, Japan) were taken.

Statistical analysis

Data were obtained from at least three separate experiments and analyzed by GraphPad prism 7.0 (GraphPad

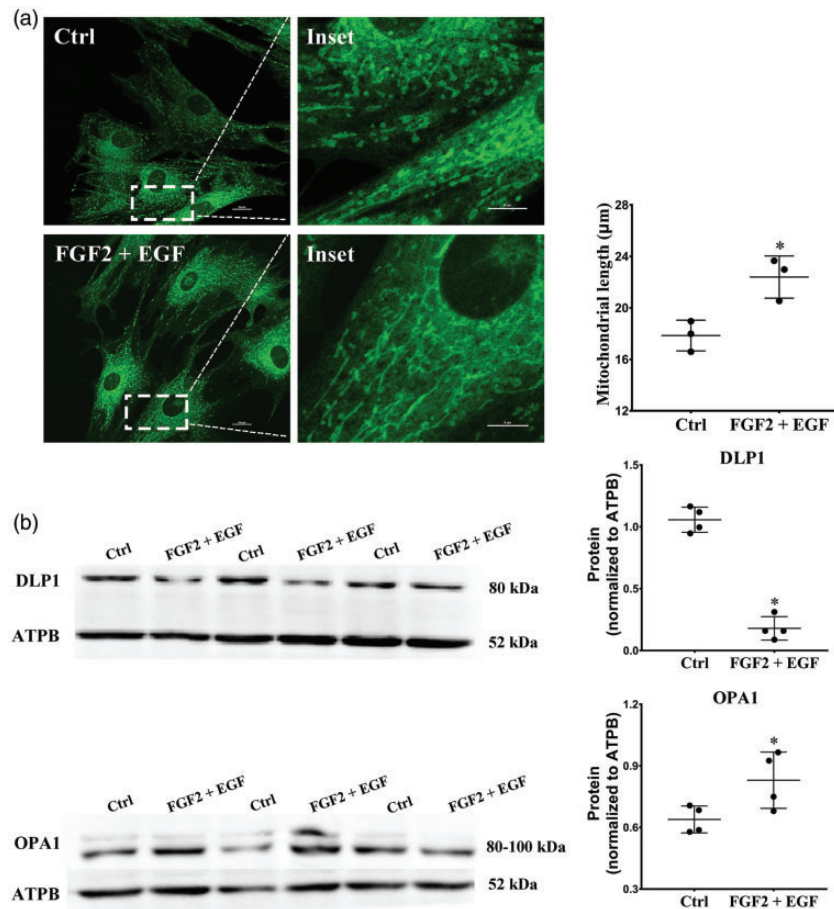


Figure 3. Reduced mitochondrial fission in differentiation state of BMSCs. (a) Mitochondrial length in differentiation state of BMSCs; mitochondria in control group or FGF2 + EGF group were stained with MitoTracker Green for 30 min and observed by confocal microscopy. Scale bars represent 10 μm (left) and 5 μm (right), original magnification $\times 2000$ (left), $\times 4000$ (right). Morphometric analysis of mitochondrial length was obtained from three independent experiments and at least 10 cells were observed in each experiment. Mitochondrial length was analyzed by Image J Software. Data were compared using unpaired Student's *t*-test. Bar graph values are mean \pm SEM. *Significantly different from control ($P < 0.05$). (b) Western blotting analysis of DLP1 and OPA1 protein contents. The Western blotting procedure was repeated four times with new set of samples obtained from separate experiments. Protein contents were analyzed by Image-Pro Plus software. Data were compared using unpaired Student's *t*-test. Bar graph values are mean \pm SEM. *Significantly different from control ($P < 0.05$). (A color version of this figure is available in the online journal.)

Software, USA). All data were presented as mean \pm SEM. The differences were determined using unpaired Student's *t*-test and $P < 0.05$ was considered statistically significant.

Results

Characterization of the isolated BMSCs

As shown in Figure 1(a), flow cytometry analysis defined a high level of expression of surface antigen CD54 or CD90, and an insignificant expression of hematopoietic antigen CD34, also a low level of leukocyte common antigen CD45, indicating the high purity of the isolated BMSCs. The purity of the BMSCs was further confirmed by the detection of the nuclear transcription factor Sox-2, which was expressed widely in

these cells (Figure 1(b)). Moreover, these cells exhibited great potential to be induced into osteocytes, adipocytes, or chondrocytes under respective culture conditions (Figure 1(c), (d), and (e)).

Reduced mitochondrial fission in differentiation state of BMSCs

FGF2 and EGF are growth factors that are known to stimulate differentiation of stem cells.^{25,26} After treatment with FGF2 and EGF, cells with high levels of CD90 and CD54 (stemness markers) were decreased (Figure 2(a)). Correspondingly, the potency of BMSCs to be induced into osteocytes or adipocytes was also decreased significantly (Figure 2(b) and (c)), indicating a successful induction of differentiation state of BMSCs by FGF2 and EGF

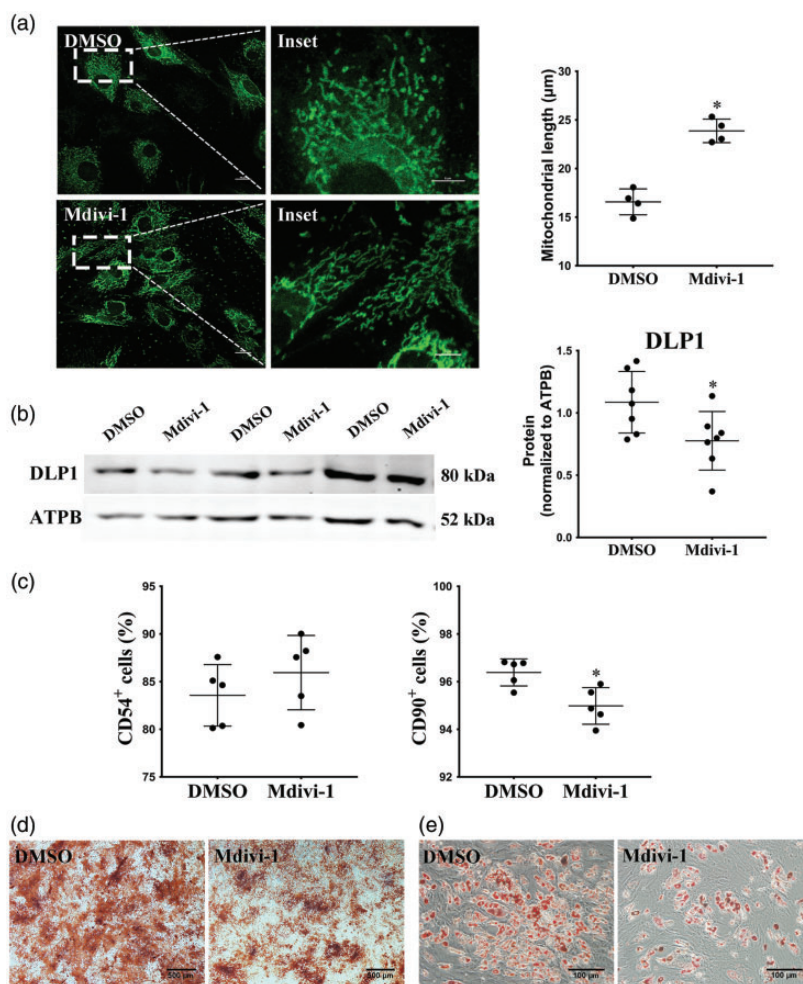


Figure 4. Reduced stemness of BMSCs by suppression of mitochondrial fission. BMSCs were treated with DMSO or 50 μ M Mdivi-1 for 6 h before harvested; (a) Mitochondria in DMSO group or Mdivi-1 group were stained with MitoTracker Green for 30 min and observed by confocal microscopy. Scale bars represent 10 μ m (left) and 5 μ m (right), original magnification $\times 2000$ (left), $\times 4000$ (right). Morphometric analysis of mitochondrial length was obtained from four independent experiments and at least 10 cells were observed in each experiment. Mitochondrial length was analyzed by Image J Software. Data were compared using unpaired Student's *t*-test. Bar graph values are mean \pm SEM. *Significantly different from control ($P < 0.05$). (b) Western blotting analysis of DLP1 protein content. The western blotting procedure was repeated seven times with a new set of samples obtained from separate experiments. Protein contents were analyzed by Image-Pro Plus software. Data were compared using unpaired Student's *t*-test. Bar graph values are mean \pm SEM. *Significantly different from control ($P < 0.05$). (c) Quantification of the fluorescence intensity of stemness markers (CD54, CD90) of BMSCs. All data were obtained from five independent experiments. Bar graph values are mean \pm SEM. *Significantly different from the control group ($P < 0.05$). (d) Osteogenic induction of BMSCs detected by Alizarin red S staining. Scale bars represent 500 μ m, original magnification $\times 40$. (e) Adipogenic induction of BMSCs detected by Oil Red O staining. Scale bars represent 100 μ m, original magnification $\times 200$. (A color version of this figure is available in the online journal.)

treatment. Under this condition, mitochondrial length was increased, indicating a decrease in mitochondrial fission during differentiation (Figure 3(a)).

To further confirm the changes in mitochondrial dynamics in the differentiation state of BMSCs, the protein content of mitochondrial fission protein DLP1 and mitochondrial fusion protein OPA1 were detected by Western blotting. As shown in Figure 3(b), DLP1 expression in the isolated mitochondria was significantly decreased after FGF2 and EGF treatment. In contrast, mitochondrial fusion protein, OPA1, was significantly increased.

Mitochondrial fission and maintenance of the stemness of BMSCs

To investigate the relationship between mitochondrial fission and the stemness of BMSCs, Mdivi-1 was used to specifically inhibit mitochondrial fission. As shown in Figure 4

(a) and (b), after the Mdivi-1 treatment, mitochondrial length was increased, along with a reduction of DLP1, indicating the effectiveness of Mdivi-1 to inhibit mitochondrial fission. Flow cytometry analysis showed that Mdivi-1 decreased stemness marker CD90 (Figure 4(c)), although no significant difference in stemness marker CD54 expression was detected in our experiments (Figure 4(c)). In addition, the potency of the osteogenic/adipogenic induction of BMSCs was also decreased significantly (Figure 4(d) and (e)).

To confirm the contribution of mitochondrial fission to the maintenance of BMSCs' stemness, mitochondrial fission accelerant TA9 was used to induce mitochondrial fission in the BMSCs. As shown in Figure 5(a) and (b), mitochondrial length was decreased along with an increased level of DLP1 content after the TA9 treatment, confirming that TA9 promoted mitochondrial fission. Flow cytometry analysis showed stronger expression of

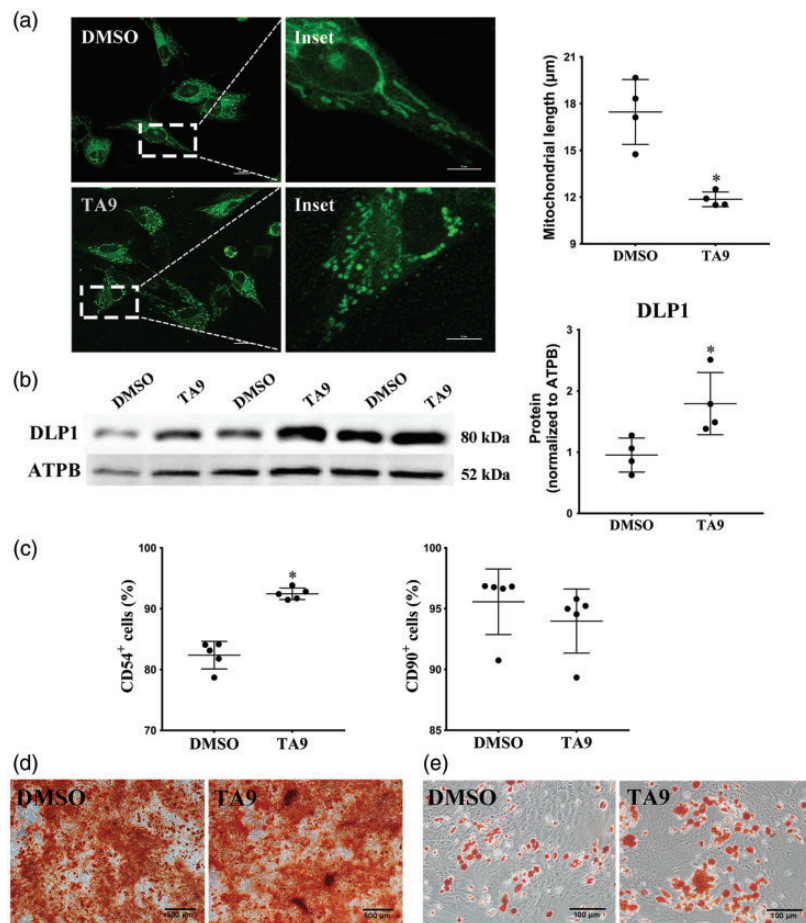


Figure 5. The association of mitochondrial fission with the maintenance of the stemness of BMSCs. BMSCs were treated with DMSO or 1 $\mu\text{mol/L}$ tyrphostin A9 (TA9) for 24 h before harvested; (a) mitochondria in DMSO group or TA9 group were stained with MitoTracker Green for 30 min and observed by confocal microscopy. Scale bars represent 10 μm (left) and 5 μm (right), original magnification $\times 2000$ (left), $\times 4000$ (right). Morphometric analysis of mitochondrial length was obtained from four independent experiments and at least 10 cells were observed in each experiment. Mitochondrial length was analyzed by Image J Software. Data were compared using unpaired Student's *t*-test. Bar graph values are mean \pm SEM. *Significantly different from control ($P < 0.05$). (b) Western blotting analysis of DLP1 protein content. The Western blotting procedure was repeated four times with new set of samples obtained from separate experiments. Protein contents were analyzed by Image-Pro Plus software. Data were compared using unpaired Student's *t*-test to analyze the difference from the control group. Bar graph values are mean \pm SEM. *Significantly different from control ($P < 0.05$). (c) Quantification of the fluorescence intensity of stemness markers (CD54, CD90) of BMSCs. All data were obtained from five independent experiments. Bar graph values are mean \pm SEM. *Significantly different from the control group ($P < 0.05$). (d) Osteogenic induction of BMSCs detected by Alizarin red S staining. Scale bars represent 500 μm , original magnification $\times 40$. (e) Adipogenic induction of BMSCs detected by Oil Red O staining scale bars represents 100 μm , original magnification $\times 200$. (A color version of this figure is available in the online journal.)

stemness marker CD54 after TA9 treatment (Figure 5(c)), while the expression of stemness marker CD90 was not changed (Figure 5(c)). The potency of BMSCs to be induced into adipocytes or osteocytes was also increased, as shown in Figure 5(d) and (e).

Discussion

The features of multilineage potential and reproducibility make BMSCs excellent candidates for cell-based therapy. Since BMSCs cultured *in vitro* have the tendency to differentiate spontaneously, it is necessary to attempt to maintain the stemness of BMSCs in cultures. Among the factors studied, mitochondrial dynamics was reported to play a fundamental role in self-renewal and differentiation of stem cells both *in vivo* and *in vitro*.^{14,27,28} However, the relationship between mitochondrial dynamics and the maintenance of stemness was unknown. Here, we demonstrated that mitochondrial fission is likely involved in the maintenance of BMSCs' stemness.

FGF2 and EGF are growth factors that are known to stimulate differentiation of neural stem/progenitor cells (NSPCs).^{25,26} Consistent with the reported effects, FGF2 and EGF treatment decreased the stemness of BMSCs as evidenced by the reduction of the percentages of CD54/CD90 positive cells and the reduced potential of BMSCs to be induced into adipocytes or osteocytes. In association with the differentiation, the elongated and interconnected mitochondria became dominant, as had been previously reported in P19 cells, embryonic stem cells, and hematopoietic stem cells.^{29–33} Moreover, the mitochondrial fission protein, DLP1, was significantly decreased, whereas the fusion protein, OPA1, was remarkably increased, demonstrating the suppression of mitochondrial fission during stem cell differentiation.

Mitochondrial fission inhibited by Mdivi-1 decreased the expression of stemness marker CD90, indicating that the stemness of BMSCs was reduced. On the other hand, mitochondrial fission promoted by TA9 enhanced the expression of stemness marker CD54, indicating that the stemness of BMSCs was increased. The changes of BMSCs' stemness was further verified by osteogenic/adipogenic induction approaches. The different changes in expression of CD54 and CD90 might lie in the different mechanisms of Mdivi-1 and TA9 in regulation of mitochondrial fission.

By inhibiting or promoting mitochondrial fission, we demonstrated that mitochondrial fission played a critical role in maintaining the stemness of BMSCs, agreeing with previous studies that showed that prevention of mitochondrial fission imposed by Mdivi-1 decreased the mammosphere-forming capacity of stem-like cells and disrupted the self-renewal of iPSCs.^{14,34} The present study also agrees with a previous study that the phospho-mimetic mutant DLP1 (pDLP1^{S592E}), an active form of DLP1, rescued the stemness of NSPC after their differentiation had been induced by Nestin knockdown.³⁵

However, controversial results regarding the effects of mitochondrial fission on cell differentiation have been published. A study using cultured neural stem cells showed that mitochondrial fission achieved by conditional genetic

deletion of MFN1/2 resulted in a lack of neurosphere formation in the cells. Furthermore, the MFN1/2 DKO mice exhibited a significant reduction of uncommitted neural stem cells and an enhancement in the percentage of committed neural progenitors.²⁷ It is possible that other mechanisms caused by MFN1/2 deletion may have compensated for the stemness maintenance effects of mitochondrial fission. Also, the reason for these contrasting findings might lie in the differing experimental systems used in these studies or the severity of stimuli.

It has been reported that the transformation of mitochondrial oxidative phosphorylation (OXPHOS) to glycolysis is critical in the maintenance of stemness;^{30,36–38} it is possible that the maintenance of the stemness of BMSCs by mitochondrial fission is achieved by enhancing glycolysis due to mitochondrial fission. This was demonstrated to promote glycolysis in previous studies.^{39–41} However, the underlying mechanisms remain to be identified.

Our results demonstrated that mitochondrial fission was involved in the maintenance of BMSCs' stemness, providing an insight into the fundamental mechanism of stem cell self-renewal and differentiation. Promoting mitochondrial fission thus may offer an alternative approach to maintaining the stemness of cells in stem cell-based therapies.

Authors' contributions: All authors participated in the experimental design, analysis of the data, interpretation of the results, and review of the manuscript. XRF carried out the experiments; XRF, YJK, WJZ, and WY wrote the manuscript.

ACKNOWLEDGMENTS

The authors thank Lin Bai and Yan Wang for providing technical assistance for mitochondrial imaging and flow cytometry analyzing, respectively.

DECLARATION OF CONFLICTING INTERESTS

The author(s) declared no potential conflicts of interest with respect to the research, authorship, and/or publication of this article.

FUNDING

The author(s) disclosed receipt of the following financial support for the research, authorship, and/or publication of this article: This work was supported by National Science Foundation of China (grant number 81230004, 81600214).

ORCID iD

Y James Kang  <http://orcid.org/0000-0001-8449-7904>

REFERENCES

1. Pittenger MF, Mackay AM, Beck SC, Jaiswal RK, Douglas R, Mosca JD, Moorman MA, Simonetti DW, Craig S, Marshak DR. Multilineage potential of adult human mesenchymal stem cells. *Science* 1999;284:143–7
2. Meirelles Lda S, Fontes AM, Covas DT, Caplan AI. Mechanisms involved in the therapeutic properties of mesenchymal stem cells. *Cytokine Growth Factor Rev* 2009;20:419–27

3. Oh SH, Witek RP, Bae SH, Zheng D, Jung Y, Piscaglia AC, Petersen BE. Bone marrow-derived hepatic oval cells differentiate into hepatocytes in 2-acetylaminofluorene/partial hepatectomy-induced liver regeneration. *Gastroenterology* 2007;**132**:1077–87
4. Berger MG, Chassagne J. [Bone marrow mesenchymal stem cells: from characterization to therapeutic use in adults and children]. *Bull Cancer* 2003;**90**:771–8
5. da Silva Meirelles L, Caplan AI, Nardi NB. In search of the in vivo identity of mesenchymal stem cells. *Stem Cells* 2008;**26**:2287–99
6. Breitbach M, Bostani T, Roell W, Xia Y, Dewald O, Nygren JM, Fries JW, Tiemann K, Bohlen H, Hescheler J, Welz A, Bloch W, Jacobsen SE, Fleischmann BK. Potential risks of bone marrow cell transplantation into infarcted hearts. *Blood* 2007;**110**:1362–9
7. Peltari K, Winter A, Steck E, Goetzke K, Hennig T, Ochs BG, Aigner T, Richter W. Premature induction of hypertrophy during in vitro chondrogenesis of human mesenchymal stem cells correlates with calcification and vascular invasion after ectopic transplantation in SCID mice. *Arthritis Rheum* 2006;**54**:3254–66
8. Rombouts WJ, Ploemacher RE. Primary murine MSC show highly efficient homing to the bone marrow but lose homing ability following culture. *Leukemia* 2003;**17**:160–70
9. Takahashi K, Yamanaka S. Induction of pluripotent stem cells from mouse embryonic and adult fibroblast cultures by defined factors. *Cell* 2006;**126**:663–76
10. Zeng L, Cai C, Li S, Wang W, Li Y, Chen J, Zhu X, Zeng YA. Essential roles of Cyclin Y-like 1 and Cyclin Y in dividing Wnt-responsive mammary stem/progenitor cells. *PLoS Genet* 2016;**12**:e1006055
11. Li S, Wang M, Chen X, Li SF, Li-Ling J, Xie HQ. Inhibition of osteogenic differentiation of mesenchymal stem cells by copper supplementation. *Cell Prolif* 2014;**47**:81–90
12. Weissleder C, Fung SJ, Wong MW, Barry G, Double KL, Halliday GM, Webster MJ, Weickert CS. Decline in proliferation and immature neuron markers in the human subependymal zone during aging: relationship to EGF- and FGF-related transcripts. *Front Aging Neurosci* 2016;**8**:274
13. Mitra K. Mitochondrial fission-fusion as an emerging key regulator of cell proliferation and differentiation. *Bioessays* 2013;**35**:955–64
14. Katajisto P, Dohla J, Chaffer CL, Pentimikko N, Marjanovic N, Iqbal S, Zoncu R, Chen W, Weinberg RA, Sabatini DM. Stem cells. Asymmetric apportioning of aged mitochondria between daughter cells is required for stemness. *Science* 2015;**348**:340–3
15. Huang YZ, Cai JQ, Xue J, Chen XH, Zhang CL, Li XQ, Yang ZM, Huang YC, Deng L. The poor osteoinductive capability of human acellular bone matrix. *Int J Artif Organs* 2012;**35**:1061–9
16. Sternecker J, Hoing S, Scholer HR. Concise review: Oct4 and more: the reprogramming expressway. *Stem Cells* 2012;**30**:15–21
17. Darabi S, Tiraihi T, Ruintan A, Abbaszadeh HA, Delshad A, Taheri T. Polarized neural stem cells derived from adult bone marrow stromal cells develop a rosette-like structure. *In Vitro Cell Dev Biol Anim* 2013;**49**:638–52
18. Fu Q, Zhang Q, Jia LY, Fang N, Chen L, Yu LM, Liu JW, Zhang T. Isolation and characterization of rat mesenchymal stem cells derived from granulocyte colony-stimulating factor-mobilized peripheral blood. *Cells Tissues Organs* 2016;**201**:412–422
19. Liu P, Feng Y, Dong C, Yang D, Li B, Chen X, Zhang Z, Wang Y, Zhou Y, Zhao L. Administration of BMSCs with muscone in rats with gentamicin-induced AKI improves their therapeutic efficacy. *PLoS One* 2014;**9**:e97123
20. Barry FP, Murphy JM. Mesenchymal stem cells: clinical applications and biological characterization. *Int J Biochem Cell Biol* 2004;**36**:568–84
21. Caplan AI, Bruder SP. Mesenchymal stem cells: building blocks for molecular medicine in the 21st century. *Trends Mol Med* 2001;**7**:259–64
22. Dominici M, Le Blanc K, Mueller I, Slaper-Cortenbach I, Marini F, Krause D, Deans R, Keating A, Prockop D, Horwitz E. Minimal criteria for defining multipotent mesenchymal stromal cells. The International Society for Cellular Therapy position statement. *Cytotherapy* 2006;**8**:315–7
23. Yin W, Li R, Feng X, James Kang Y. The involvement of cytochrome c oxidase in mitochondrial fusion in primary cultures of neonatal rat cardiomyocytes. *Cardiovasc Toxicol* 2018;**18**:365–73
24. Wang B, Dong D, Kang YJ. Copper chaperone for superoxide dismutase-1 transfers copper to mitochondria but does not affect cytochrome c oxidase activity. *Exp Biol Med* 2013;**238**:1017–23
25. Zhou S, Ochalek A, Szczesna K, Avci HX, Kobolak J, Varga E, Rasmussen M, Holst B, Cirera S, Hyttel P, Freude KK, Dinnyes A. The positional identity of iPSC-derived neural progenitor cells along the anterior-posterior axis is controlled in a dosage-dependent manner by bFGF and EGF. *Differentiation* 2016;**92**:183–94
26. Itoh N, Ohta H, Nakayama Y, Konishi M. Roles of FGF signals in heart development, health, and disease. *Front Cell Dev Biol* 2016;**4**:110
27. Khacho M, Clark A, Svoboda DS, Azzi J, MacLaurin JG, Meghaizel C, Sesaki H, Lagace DC, Germain M, Harper ME, Park DS, Slack RS. Mitochondrial dynamics impacts stem cell identity and fate decisions by regulating a nuclear transcriptional program. *Cell Stem Cell* 2016;**19**:232–47
28. Folmes CD, Ma H, Mitalipov S, Terzic A. Mitochondria in pluripotent stem cells: stemness regulators and disease targets. *Curr Opin Genet Dev* 2016;**38**:1–7
29. Vega-Naredo I, Loureiro R, Mesquita KA, Barbosa IA, Tavares LC, Branco AF, Erickson JR, Holy J, Perkins EL, Carvalho RA, Oliveira PJ. Mitochondrial metabolism directs stemness and differentiation in P19 embryonal carcinoma stem cells. *Cell Death Differ* 2014;**21**:1560–74
30. Simsek T, Kocabas F, Zheng J, Deberardinis RJ, Mahmoud AI, Olson EN, Schneider JW, Zhang CC, Sadek HA. The distinct metabolic profile of hematopoietic stem cells reflects their location in a hypoxic niche. *Cell Stem Cell* 2010;**7**:380–90
31. St John JC, Ramalho-Santos J, Gray HL, Petrosko P, Rawe VY, Navara CS, Simerly CR, Schatten GP. The expression of mitochondrial DNA transcription factors during early cardiomyocyte in vitro differentiation from human embryonic stem cells. *Cloning Stem Cells* 2005;**7**:141–53
32. Xu X, Duan S, Yi F, Ocampo A, Liu GH, Izpisua Belmonte JC. Mitochondrial regulation in pluripotent stem cells. *Cell Metab* 2013;**18**:325–32
33. Zhang J, Khvorostov I, Hong JS, Oktay Y, Vergnes L, Nuebel E, Wahjudi PN, Setoguchi K, Wang G, Do A, Jung HJ, McCaffery JM, Kurland IJ, Reue K, Lee WN, Koehler CM, Teitell MA. UCP2 regulates energy metabolism and differentiation potential of human pluripotent stem cells. *Embo J* 2011;**30**:4860–73
34. Vazquez-Martin A, Cufi S, Corominas-Faja B, Oliveras-Ferreros C, Vellon L, Menendez JA. Mitochondrial fusion by pharmacological manipulation impedes somatic cell reprogramming to pluripotency: new insight into the role of mitophagy in cell stemness. *Aging* 2012;**4**:393–401
35. Wang J, Huang Y, Cai J, Ke Q, Xiao J, Huang W, Li H, Qiu Y, Wang Y, Zhang B, Wu H, Zhang Y, Sui X, Bardeesi ASA, Xiang AP. A Nestin-cyclin-dependent kinase 5-dynamin-related protein 1 axis regulates neural stem/progenitor cell stemness via a metabolic shift. *Stem Cells* 2018;**36**:589–601
36. Enomoto K, Watanabe-Susaki K, Kowno M, Takada H, Intoh A, Yamanaka Y, Hirano H, Sugino H, Asashima M, Kurisaki A. Identification of novel proteins differentially expressed in pluripotent embryonic stem cells and differentiated cells. *J Med Invest* 2015;**62**:130–6
37. Hsu YC, Wu YT, Yu TH, Wei YH. Mitochondria in mesenchymal stem cell biology and cell therapy: from cellular differentiation to mitochondrial transfer. *Semin Cell Dev Biol* 2016;**52**:119–31
38. Zhang J, Nuebel E, Daley GQ, Koehler CM, Teitell MA. Metabolic regulation in pluripotent stem cells during reprogramming and self-renewal. *Cell Stem Cell* 2012;**11**:589–95

39. Mishra P, Chan DC. Metabolic regulation of mitochondrial dynamics. *J Cell Biol* 2016;**212**:379–87
40. Hagenbuchner J, Kuznetsov AV, Obexer P, Ausserlechner MJ. BIRC5/Survivin enhances aerobic glycolysis and drug resistance by altered regulation of the mitochondrial fusion/fission machinery. *Oncogene* 2013;**32**:4748–57
41. Guido C, Whitaker-Menezes D, Lin Z, Pestell RG, Howell A, Zimmers TA, Casimiro MC, Aquila S, Ando S, Martinez-Outschoorn UE, Sotgia F, Lisanti MP. Mitochondrial fission induces glycolytic reprogramming in cancer-associated myofibroblasts, driving stromal lactate production, and early tumor growth. *Oncotarget* 2012;**3**:798–810

(Received November 9, 2018, Accepted December 2, 2018)